

# Seismic shear force magnification in RC cantilever structural walls, designed according to Eurocode 8

Klemen Rejec · Tatjana Isaković · Matej Fischinger

Received: 24 September 2010 / Accepted: 5 June 2011 / Published online: 18 June 2011  
© Springer Science+Business Media B.V. 2011

**Abstract** The paper contains a discussion of the inelastic dynamic magnification of seismic shear forces in cantilever walls with rectangular cross-sections. An extensive parametric study was performed in order to determine the reliability of the procedure in Eurocode 8 (EC8). A large number of single cantilever walls which are characteristic for the design practice in Europe and designed to satisfy all the EC8 requirements were analysed. The results obtained with the (modified) code procedures were compared with the results of inelastic response history analyses. If properly applied, the EC8 procedure for DCH walls usually yields good results for the base shears. However, as presently formulated and understood in the EC8, it can yield significantly incorrect results (overestimations of up to 40%). For this reason three modifications were introduced: (1) Keintzel's formula, which is adopted in EC8, should be used in combination with the seismic shears obtained by considering the first mode of the excitation only; (2) the upper limit of the shear magnification factor should be related to the total shear force; and (3) a variable shear magnification factor along the height of the wall should be applied. The present procedure in EC8 for DCM structures (using a constant shear magnification factor of 1.5 for all walls) is non-conservative. For DCM walls it is strongly recommended that the same procedure as required for DCH walls be used.

**Keywords** Reinforced concrete walls · Seismic shear forces · Eurocode 8 · Shear magnification factors · Inelastic response history analyses · Lumped plasticity model

---

K. Rejec (✉) · T. Isaković · M. Fischinger  
Faculty of Civil and Geodetic Engineering, University of Ljubljana, Jamova 2, 1000 Ljubljana, Slovenia  
e-mail: klemen.rejec@ikpir.fgg.uni-lj.si

T. Isaković  
e-mail: tisak@ikpir.fgg.uni-lj.si

M. Fischinger  
e-mail: matej.fischinger@ikpir.fgg.uni-lj.si

## 1 Introduction

At the design level, the actual shear forces in reinforced concrete structural walls due to seismic loads are, typically, considerably higher than the forces foreseen by the equivalent linear-elastic lateral force analysis, or by the modal response spectrum analysis specified in the codes. Simply said, this magnification occurs due to flexural overstrength and the amplified effect of the higher modes in the inelastic range. This seismic shear magnification phenomenon, which was first documented by [Blakeley et al. \(1975\)](#), can lead to the brittle shear failure of the walls. A possible enlargement of seismic shear demands caused by dynamic effects was also indicated in the response of a full scale 7-storey RC structural wall tested on a shake table at University of California, San Diego ([Panagiotou et al. 2007](#)). An effective design procedure which could be used to assess the realistic shear demand in RC structural walls is therefore needed.

The Eurocode design provisions ([CEN 2004](#)) provide a related shear magnification factor  $\varepsilon$ , which is used to multiply the values obtained by the linear-elastic lateral force or modal response spectrum analysis. For ductility class medium (DCM) walls, a simple constant factor  $\varepsilon = 1.5$  is used. For walls which enter far into the inelastic range (ductility class high—DCH structures), larger shear magnifications are expected, and the factor  $\varepsilon$  should be calculated using the expression proposed by [Keintzel \(1990\)](#), which explicitly takes into account the effect of higher modes in the inelastic range and flexural overstrength as explained in [Fardis \(2009\)](#). However, recent research work performed by [Rutenberg and Nsieri \(2006\)](#), [Kappos and Antoniadis \(2007\)](#) and [Priestley et al. \(2007\)](#) has shown that the Eurocode procedure needs some modifications in order to provide an improved estimate of shear magnification factors. In particular, the work of Rutenberg and Nsieri has demonstrated that the  $\varepsilon$  factor is too low for DCM walls, and is also frequently conservative for DCH walls.

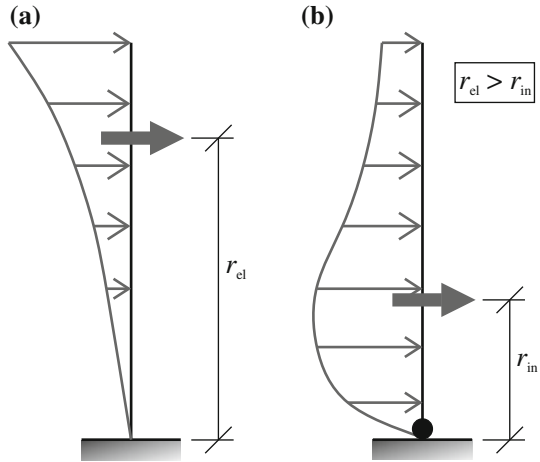
Kentzel's research was certainly up-to-date in the time when it was published, but the supporting parameter study was rather limited with respect to the criteria of modern earthquake engineering. For this reason an extensive parametric study of the inelastic response of multi-storey cantilever structural walls, designed according to Eurocode 8 ([CEN 2004](#)), was performed in order to determine the reliability of the Eurocode procedure for the determination of seismic shear demand in structural walls. The geometric characteristics of the walls were carefully chosen to represent realistic construction practice. Whereas Keintzel's expression (if properly applied) was found to be adequate in many cases, some shortcomings in such an application were identified, and further improvements of the  $\varepsilon$  factor are proposed in the paper.

## 2 Magnification of seismic shear forces in cantilever walls

### 2.1 General description of the problem

It is assumed that the Eurocode 8 (EC8) design procedure confines yielding of the longitudinal reinforcement to the section at the base of the multi-storey cantilever wall (no plastic hinges are expected in the upper stories). After a plastic hinge has formed at the base of the wall, the inelastic wall may be interpreted as an equivalent elastic system (e.g. considering the secant stiffness) when discussing the vibration modes and related seismic forces. During the inelastic response the influence of the higher modes on shear demand is amplified in comparison with the first mode contribution (see Sect. 2.2). This lowers the position of the resultant of the seismic forces, making it closer to the base of the wall (Fig. 1). With the

**Fig. 1** Lateral seismic forces distribution corresponding to an **a** elastic and **b** inelastic response of a cantilever wall



given bending moment at the base, which is equal to the flexural capacity of the wall, it is clear that the resultant seismic force (i.e. the shear force) will increase.

## 2.2 Factors contributing to the shear force magnification

### 2.2.1 The influence of overstrength

A consideration of simple equilibrium shows that flexural overstrength (i.e. the ratio between the actual flexural resistance and the design bending moment) increases the design seismic shear forces. The increase is predominantly related to the first mode response (see also Sect. 2.2.3 and “Appendix”).

### 2.2.2 Influence of the period shift

By analysing the vibration modes of an equivalent elastic system representing a hinged wall, it can be observed that after a plastic hinge is formed at the base the first mode shape and period significantly change while the higher mode characteristics remain practically unchanged.

Due to the softening of the structural wall in the inelastic range, the first mode spectrum value typically diminishes, whereas the spectrum values for the higher modes remain on the plateau of the spectrum. The relative influence of the higher modes therefore increases in the inelastic range.

### 2.2.3 Amplified influence of the higher modes

The first mode seismic forces contribute most of the overall seismic moment at the base of the wall, which is limited by its flexural resistance (see also Fig. 17 in “Appendix”). Energy dissipation is therefore predominantly limited to the flexural response in the first mode. Consequently, the first mode shear forces are reduced due to the energy dissipating mechanism, whereas the shear forces due to the higher modes are not. This significantly increases the relative contribution of the higher modes to the shear force which occurs during the inelastic response.

### 3 The Eurocode procedure

Eurocode 8 requires that the shear forces obtained by the equivalent elastic analysis  $V'_{Ed}$  are multiplied (over the complete height of the wall) by the shear magnification factor  $\varepsilon$ , in order to obtain the design shear forces  $V_{Ed}$ :

$$V_{Ed} = \varepsilon \cdot V'_{Ed} \tag{1}$$

In the case of DCM structures, this shear magnification factor can be simply taken as  $\varepsilon = 1.5$ .

For DCH walls (which enter far into the inelastic range), the shear magnification factor is calculated from the expression (2) that was originally proposed by Keintzel (1990):

$$\varepsilon = q \cdot \sqrt{\left(\frac{\gamma_{Rd}}{q} \cdot \frac{M_{Rd}}{M_{Ed}}\right)^2 + 0.1 \cdot \left(\frac{S_e(T_C)}{S_e(T_1)}\right)^2} \begin{cases} \leq q \\ \geq 1.5 \end{cases} \tag{2}$$

where:

- $q$  is the behaviour (seismic force reduction) factor used in the design;
- $M_{Ed}$  is the design bending moment at the base of the wall;
- $M_{Rd}$  is the design flexural resistance at the base of the wall;
- $\gamma_{Rd}$  is the factor to account for overstrength due to steel strain-hardening;
- $T_1$  is the fundamental period of vibration of the building in the direction of shear forces;
- $T_C$  is the upper limit period of the constant spectral acceleration region of the spectrum;
- $S_e(T)$  is the ordinate of the elastic response spectrum.

The background of expression (2) is given below (see also “Appendix”).

Keintzel (1990) performed a parametric study, comparing the results obtained by means of the equivalent elastic code procedure and inelastic response history analyses. Based on the results of this study, he assumed that modal combination can also be applied in the inelastic range, and that only the contribution of the first two modes is important (see also Fig. 17b in “Appendix”):

$$V_{Ed}^* = \sqrt{\left(V'_{Ed,1}\right)^2 + \left(V'_{Ed,2}\right)^2} \tag{3}$$

where:

- $V_{Ed}^*$  is the design seismic shear at the base of the wall as defined by Keintzel;
- $V'_{Ed,1}$  is the seismic shear at the base of the wall due to the first mode;
- $V'_{Ed,2}$  is the seismic shear at the base of the wall due to the second mode.

Keintzel further assumed that the level of the reduction of seismic forces belonging to each mode is proportional to the level of the seismic moment at the base of the wall contributed by the excitation of that mode. For this reason (see Fig. 17a in “Appendix”) practically only the contribution of the first mode should be reduced by  $q$  (as assumed in the standard equivalent elastic design), whereas the contribution of the second mode should be elastic/unreduced ( $q \cdot V'_{Ed,2}$ ):

$$V_{Ed}^* = \sqrt{\left(V'_{Ed,1}\right)^2 + \left(q \cdot V'_{Ed,2}\right)^2} \tag{4}$$

Considering that flexural overstrength affects only the first mode shears, and that in the response spectrum analysis the contribution of the second mode at the base is about  $\sqrt{0.1} \cdot$

$S_e(T_2)/S_e(T_1)$  (Keintzel’s research concerned only the seismic shears at the base) of the first mode (see Fig. 17c in “Appendix”), the following expression (5) can be derived:

$$V_{Ed} = V_{Ed}^* = \sqrt{\left(\frac{M_{Rd}}{M_{Ed}} \cdot \gamma_{Rd} \cdot V'_{Ed,1}\right)^2 + \left(q \cdot V'_{Ed,1} \cdot \sqrt{0.1} \cdot \frac{S_e(T_C)}{S_e(T_1)}\right)^2} \tag{5}$$

Expression (2) is obtained by removing the factor  $V'_{Ed,1} \cdot q$  out of the square root in Eq. (5):

$$V_{Ed} = V'_{Ed,1} \cdot q \cdot \sqrt{\left(\frac{\gamma_{Rd}}{q} \cdot \frac{M_{Rd}}{M_{Ed}}\right)^2 + \left(\sqrt{0.1} \cdot \frac{S_e(T_C)}{S_e(T_1)}\right)^2} = V'_{Ed,1} \cdot \varepsilon \tag{6}$$

It is important to note that according to the presented derivation Keintzel’s magnification factor should be applied to the seismic shear forces obtained by the equivalent elastic analysis, considering only the first mode of excitation. It should also be added that although the assumption  $V'_{Ed,2}/V'_{Ed,1} = \sqrt{0.1} \cdot S_e(T_2)/S_e(T_1)$  is valid only at the base of cantilever walls, EC8 imposes the application of Eq. (2) for all seismic shear forces along the entire height.

Keintzel also assumed that  $\varepsilon$  is limited by the upper value of  $q$ . The same assumption was adopted in EC8. Whereas it is true that the upper bound for  $V_{Ed}$  should be the elastic value  $V_E = q \cdot V'_{Ed}$  (as applied in EC8), the assumption in Keintzel’s original procedure that  $V_E$  equals  $V'_{Ed,1} \cdot q$ , neglecting the contribution of higher modes, is not valid. This will be further discussed in the continuation of this paper.

It is obvious that Keintzel’s derivation involves a series of quite crude assumptions and approximations. First of all, the concept valid in the elastic range is used also in the inelastic range. Since this procedure was originally validated by a very limited parametric study, a more complete study, presented in the next section, was performed.

#### 4 The parametric study: the input parameters

The actual shear magnifications were determined by the inelastic response analyses and compared with the values obtained by the EC8 (Keintzel’s) procedure as described in the previous section.

In the first stage of the study 24 walls, typical for the construction practice in Europe, were designed according to the Eurocode provisions. All of the design and minimum requirements for DCH walls were considered. The number of stories ( $n$ ) varied from 4 to 20. Within each group of walls having the same number of stories the following parameters were varied, depending on the design requirements and the feasibility of the construction:

- the length of the wall  $l_w$  (between 2 and 8 m);
- the wall-to-floor area ratio  $r_f = A_w/A_f$  (1.5, 2.0 and 2.5%).

All walls had rectangular cross sections. The thickness of the walls was  $b_w = 30$  cm and all storeys were  $h_s = 3.0$  m high.

##### 4.1 Field of application

Only the effects of shear magnification in cantilever walls have been discussed. Additional factors such as torsional effects and the influence of varying axial forces in coupled walls and dual structures were not considered. The results therefore apply only to uncoupled walls with similar lengths, which are regular in plan and elevation. It was also assumed that the EC8 design procedure precludes plastic hinging in the upper stories of the wall.

#### 4.2 Design considerations

The walls were designed according to the provisions of Eurocode 8 for ductility class high (DCH) walls, using modal response spectrum analysis and considering a behaviour factor of  $q = q_0 \cdot \alpha_u / \alpha_1 = 4.0 \cdot 1.1 = 4.4$ , representing regular flexible uncoupled wall systems. The vertical load corresponding to the seismic design situation was  $10 \text{ kN/m}^2$ . The attributed floor masses  $m_i$  and the vertical non-seismic loads  $F_i$  were determined by taking into account the wall-to-floor area ratio  $r_f = A_w / A_f$ . The requirements in the Slovenian national Annex to Eurocode 2 (CEN 2005) were also considered: (i) the minimum amount of total vertical reinforcement in the walls was  $A_{s, \text{vmin}} = 0.003 \cdot A_c$  and (ii) the minimum size of the vertical reinforcing bars in the boundary elements was 12 mm. Standard C30/37 concrete and S500 steel were used in the design.

#### 4.3 Notation of the walls and their characteristics

The analysed walls were tagged 1–24. The variation of the basic input parameters—the number of storeys ( $n$ ), the length of the wall ( $l_w$ ), and the wall-to-floor area ratio  $A_w / A_f$  are illustrated in Fig. 2a, b, where the integers on the horizontal axes represent each individual wall. As said above, the number of storeys varied from 4 to 20. The length of the walls varied from 2 to 8 m. The length of the 20-storey high wall was 8 m due to the serviceability limit state—SLS requirements. The wall-to-floor area ratio  $r_f = A_w / A_f$  varied between 1.5 and 2.5%. Combinations which did not fulfil all the EC8 requirements (including SLS) were eliminated. Each combination of the basic input parameters is reflected in the natural periods and overstrength factors, which are the key parameters in the present study. The values of the first ( $T_1$ ) and second ( $T_2$ ) periods are shown in Fig. 2c. They show that the values corresponding to  $T_2 < T_C$  ( $T_C$  is the upper limit period of the constant spectral acceleration region) and to  $T_1 > T_C$  are typical for mid-rise buildings in everyday design practice.

The flexural overstrength factors (Fig. 2d) were in most cases less than 2.0. Larger overstrength factors were observed in the case of the 6.0 m long 4-storey walls, and in the 16 and 20-storey walls for which the length of the wall had been determined by the SLS criteria. Note that the overstrength factors were calculated on the basis of the design material characteristics. Compatibly with this assumption, the overstrength factor  $\gamma_{Rd}$  in the expression (2) for the  $\varepsilon$  factor was taken as 1.0 (no overstrength due to material characteristics was considered, either in the design or in the analysis).

#### 4.4 Analytical model and analysis considerations

Modal response spectrum analyses were carried with ETABS (CSI 2009), using standard analysis parameters. The elastic flexural and shear stiffness properties equalled one-half of the corresponding stiffness of the uncracked elements. Eurocode design response spectra for  $PGA = 0.25 \text{ g}$  (design ground acceleration  $a_g = 0.25 \text{ g}$  corresponds to the zone with the highest seismic hazard in the Republic of Slovenia) and soil type C (very frequent type of soil in the Republic of Slovenia) were used. The attributed discrete floor masses  $m_i$  and the vertical non-seismic loads  $F_i$  corresponded to the attributed floor areas  $A_i$ . The values of  $m_i$  and  $F_i$  are reported in Table 1.

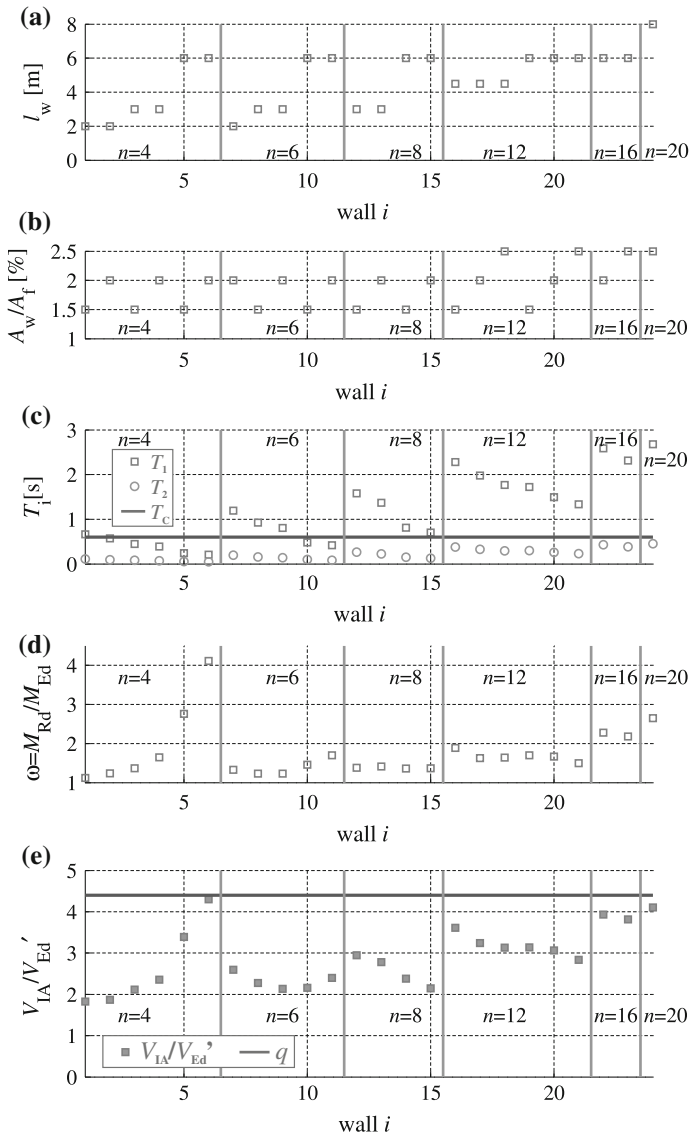


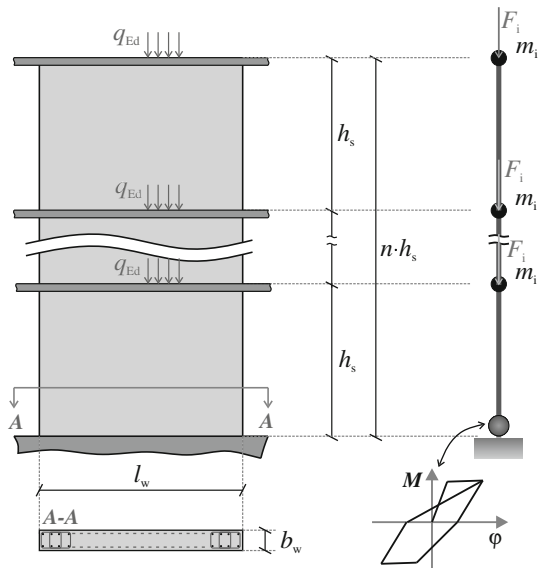
**Fig. 2** Notation of the analysed walls, the variation of the basic input parameters and the corresponding actual shear magnification: **a** lengths of the walls— $l_w$  [m]; **b** wall-to-floor ratio— $A_w/A_f$  [%]; **c** first and second periods of the walls  $T_1$ [s] and  $T_2$ [s] compared with  $T_C$ [s]; **d** overstrength factors  $\omega$ ; **e** actual shear magnifications  $V_{IA}/V'_{Ed}$

As the walls were designed to exhibit inelastic flexural deformation only at their bases, the nonlinear model was obtained by adding a nonlinear hinge controlled by bi-linear Takeda hysteresis rules at the base of the wall (Fig. 3). A separate study showed that the seismic shear force results are not significantly dependent on the choice of unloading stiffness or pinching parameters. The resulting shears varied up to 10% depending on the hysteretic parameters. The model with Takeda hysteretic rules with unloading factor  $\beta = 0.5$  yielded approximately

**Table 1** The values of the attributed floor masses  $m_i$  and vertical non-seismic loads  $F_i$  according to the notation of the walls

Wall tag $i$	1	2	3	4	5	6	7	8	9	10	11	12
$m_i$ [t]	41	31	61	46	122	92	31	61	46	122	92	61
$F_i$ [kN]	200	150	300	225	600	450	150	300	225	600	450	300
Wall tag $i$	13	14	15	16	17	18	19	20	21	22	23	24
$m_i$ [t]	46	122	92	92	69	55	122	92	73	92	73	98
$F_i$ [kN]	225	600	450	450	337	270	600	450	360	450	360	480

**Fig. 3** Analytical model for inelastic response history analysis



mean values of seismic shears. Therefore it was selected as the most appropriate for the purposes of the research. To enable proper comparisons, the same initial stiffness was chosen for the elastic and (bi-linear) inelastic models. The moment-curvature section analyses were performed in [OpenSees \(2008\)](#) in order to obtain the characteristic moments and curvatures for the wall cross section at its base. The equivalent plastic hinge length  $L_P$  was determined according to [Priestley et al. \(2007\)](#). As it is explained in [Priestley et al. \(2007\)](#), the plastic curvature should be considered as constant over  $L_P$ . This procedure also takes into account the deformations caused by the slippage of longitudinal reinforcement along the embedment in the foundation by adding the length of strain penetration in foundations  $L_{SP}$  to the total value of  $L_P$ . Design values for the material strengths were used in the response history analysis in order to facilitate comparisons with the equivalent elastic design procedures (note again that no material overstrength was considered in the calculation of the  $\varepsilon$  factor). This procedure was chosen in order to eliminate the uncertainties related to overstrength factor evaluation. Five percent mass and current stiffness proportional Rayleigh damping was considered in



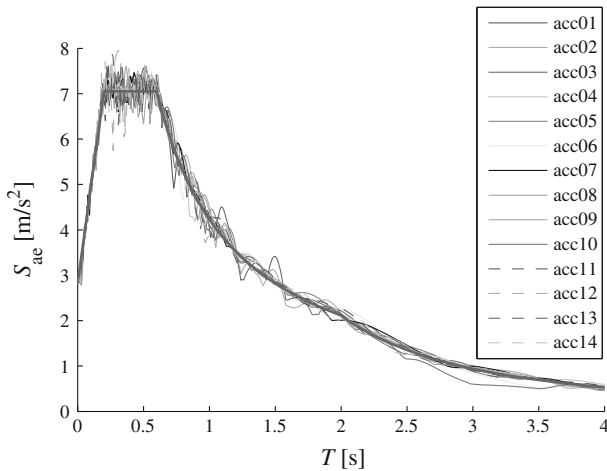


**Fig. 4** The elastic response spectra (5% damping) of 14 artificial accelerograms used in the analysis compared with the Eurocode spectrum for soil type C and  $a_g = 0.25$  g (thick line)

the first and second modes. The response history analyses were performed using [OpenSees \(2008\)](#).

#### 4.5 Input motions

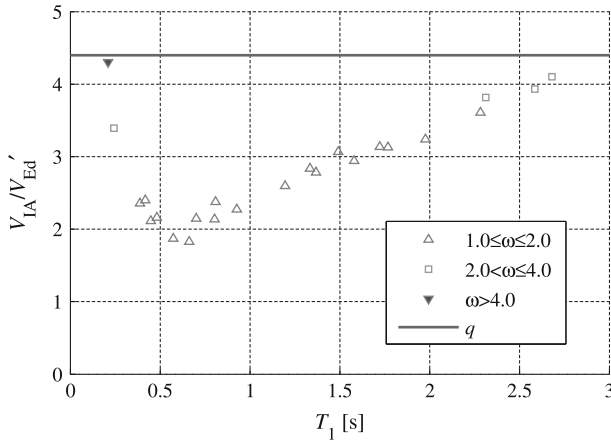
14 artificial accelerograms with spectra matching the EC8 elastic spectrum for soil type C and  $a_g = 0.25$  g were used in the response history analyses (Fig. 4). The accelerograms were generated using the program SYNTH ([Naumoski 1998](#)).

### 5 Parametric study: results for the shear magnification factors

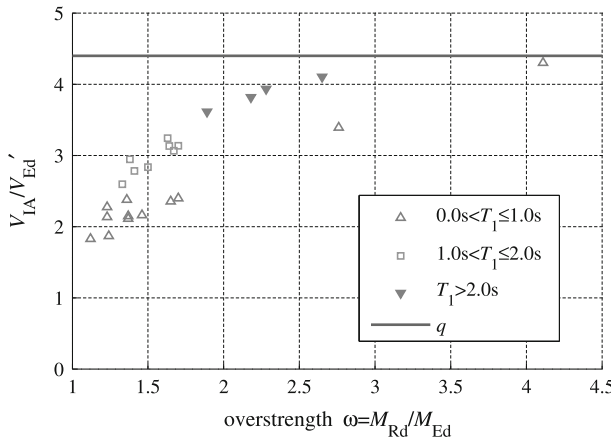
The actual shear magnification is defined by the ratio  $V_{IA}/V'_{Ed}$ .  $V'_{Ed}$  is the base shear obtained by response spectrum analysis considering all important modes (as typically considered by designers). The value  $V_{IA}$  is the mean value of the maximum seismic shear at the base of the wall, obtained by using the 14 selected accelerograms.

Figure 2e illustrates large shear magnifications, in particular for structures with longer fundamental periods and large flexural overstrengths, resulting in  $V_{IA}/V'_{Ed}$  ratios of up to 4.3. As expected, the upper value of  $V_{IA}/V'_{Ed}$  is approximately equal to the behaviour factor  $q = 4.4$ , since the upper bound for the seismic shear force should be the elastic value  $V_E = V'_{Ed} \cdot q$ . Shear magnification factors larger than 3 were calculated for the walls with 12 and more storeys, whereas the magnification coefficients for lower buildings (with the exception of 6.0 m long 4-storey walls, which have very high overstrengths) varied between 2.0 and 3.0.

The results for the shear magnification factors are further illustrated in relation to the first period  $T_1$  in Fig. 5, and the overstrength factors  $\omega = M_{Rd}/M_{Ed}$  in Fig. 6. The analyses reconfirmed that these two parameters should be taken into account when evaluating the shear magnification factors in structural walls. The results also suggest that the application of a uniform magnification factor for all types of walls (as in the case of DCM design) can lead to inappropriate estimates of the seismic shear forces.



**Fig. 5** Actual shear magnifications  $V_{IA}/V'_{Ed}$  plotted against  $T_1$



**Fig. 6** Actual shear magnifications  $V_{IA}/V'_{Ed}$  plotted against the overstrength factor

## 6 Verification of the shear magnification factors in the Eurocode

### 6.1 Verification of the EC8 procedure

The values of the EC8 seismic design shear forces at the base of the walls (denoted by  $V_{Ed} = V_{Ed,EC8}$ ) are compared with those obtained by inelastic response history analysis (denoted as  $V_{IA}$ ). The values for  $V_{Ed,EC8}$  were derived according to Eq. (1) using the seismic shear forces obtained by modal response spectrum analysis, taking into account all the important modes (denoted by  $V'_{Ed}$ ), as is common in the design practice. The normalised results  $V_{Ed,EC8}/V_{IA}$  are illustrated in Figs. 7, 8, 9 by squares.

In Fig. 7 the results are presented by wall configuration tags. It seems that the EC8 procedure works fine for the 4, 6, 16 and 20-storey walls, whereas the shear magnifications for the mid-rise 8 and 12-storey walls are considerably overestimated (up to 40% for the 12-storey wall with  $l_w = 4.5$  m and  $A_w/A_f = 2.5\%$ ). Similarly Fig. 8, which plots the

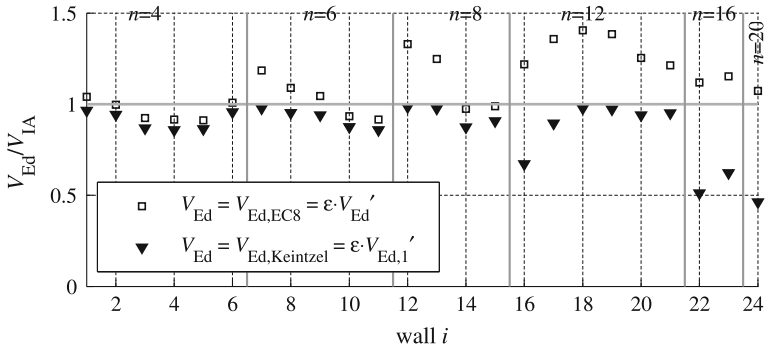


**Fig. 7** Values for  $V_{Ed,EC8}/V_{IA}$  (indicated by square markers) and  $V_{Ed,Keintzel}/V_{IA}$  (indicated by triangular markers) compared to the actual shear magnifications (shown by a grey horizontal line). Each integer on the horizontal axis denotes an analysed wall configuration

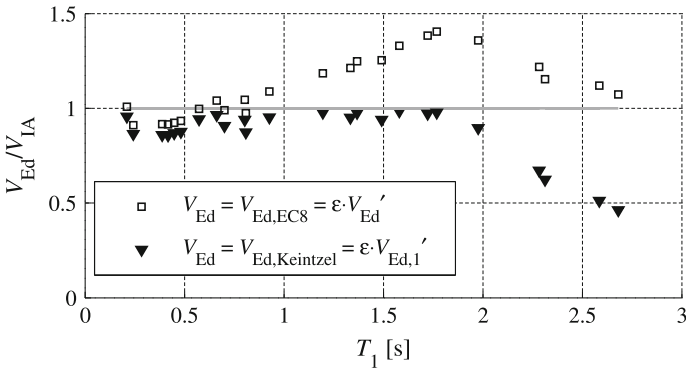


**Fig. 8** Values  $V_{Ed,EC8}/V_{IA}$  (indicated by square markers) and  $V_{Ed,Keintzel}/V_{IA}$  (indicated by triangular markers) compared to the actual shear magnifications (shown by a grey horizontal line) in relation to  $T_1$

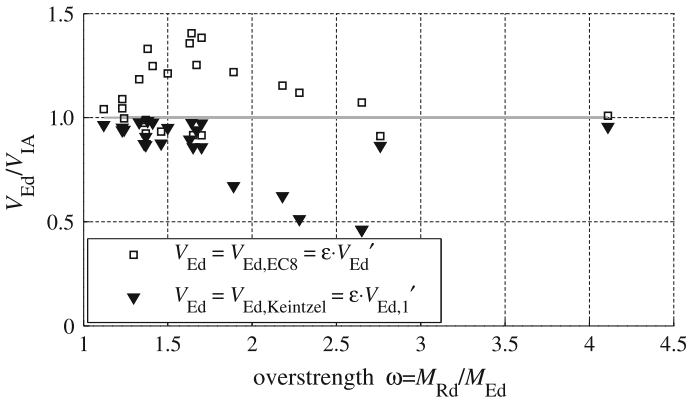


**Fig. 9** Values for  $V_{Ed,EC8}/V_{IA}$  (indicated by square markers) and  $V_{Ed,Keintzel}/V_{IA}$  (indicated by triangular markers) compared to the actual shear magnifications (shown by a grey horizontal line) in relation to the overstrength factor

relation between  $V_{Ed,EC8}/V_{IA}$  and the fundamental period  $T_1$ , suggests that EC8 works fine for walls with  $T_1 < 1.0$  s and  $T_1 > 2.5$  s. In the mid period range EC8 overestimates the shear forces.

The conservative results, which EC8 provides in the case of the mid-rise walls in the mid period range, are not difficult to explain. As noted in Sect. 3, Keintzel's formula should be used in combination with the seismic shears obtained by considering the first mode of the excitation only. Since EC8 does not specify this requirement, designers would typically follow the established practice with standard programs considering all important modes. In the case of flexible buildings (walls), where the contribution of the higher modes is important even in the elastic range, this would yield conservative results. Even greater conservatism would be expected in the case of long-period walls. However for these walls original Keintzel's procedure yields very unconservative values (the upper bound of  $\varepsilon$  is too low; see the next sub-section). These two errors compensate each other. So it seems that the EC8 procedure yields good results for flexible walls, although in reality this is the result of two wrong assumptions.

## 6.2 Verification of Keintzel's original procedure

Within Keintzel's original procedure, results (denoted by  $V_{Ed,Keintzel}$ ) are obtained by multiplying the shears taking into account only the contribution of the first mode ( $V'_{Ed,1}$ ) and magnification factor obtained by using expression (2).

The results  $V_{Ed,Keintzel}/V_{IA}$  are presented in Figs. 7, 8, 9 where they have been plotted against the walls' tags,  $T_1$ , and  $\omega$ , respectively. The figures show that Keintzel's procedure (although based on a very simple parametric study) provides a very good estimate of the shear magnifications for walls with  $T_1 < 2.0$  s. This corresponds to the analysed walls with 8 or less storeys, as well as to the 6.0 m long 12-storey walls. In other cases ( $T_1 > 2.0$  s) the actual shears are significantly underestimated. Moreover, this discrepancy increases rapidly for higher values of  $T_1$  (Fig. 8).

It has been determined that the reason for these discrepancies lies in the inappropriate formulation of the upper bound for the shear magnification factor in the Keintzel's expression. The upper bound should be defined based on the total shear force obtained by the equivalent elastic analysis (considering all important modes), and not on the shear force obtained by considering the fundamental mode only (as is consistent with Keintzel's original procedure).

## 7 Possible improvements of the procedure given in EC8

The analyses in the previous section have clearly indicated possible modifications and improvements.

First, the  $\varepsilon$  factor, as proposed by Keintzel, should be applied to the shear forces obtained by considering only the fundamental mode ( $V'_{Ed,1}$ ) in the equivalent elastic response spectrum analysis. Most modern computer codes are able to identify the contribution of the each mode separately.

However, the upper limit of the  $\varepsilon$  factor should be related to the total shear force. Considering that the seismic shear force is limited by the elastic value  $V_E$  and taking into account the first and the second modes, the upper bound of the shear force ( $\varepsilon_{upper}$  denotes the highest possible value for  $\varepsilon$ ) is defined by:

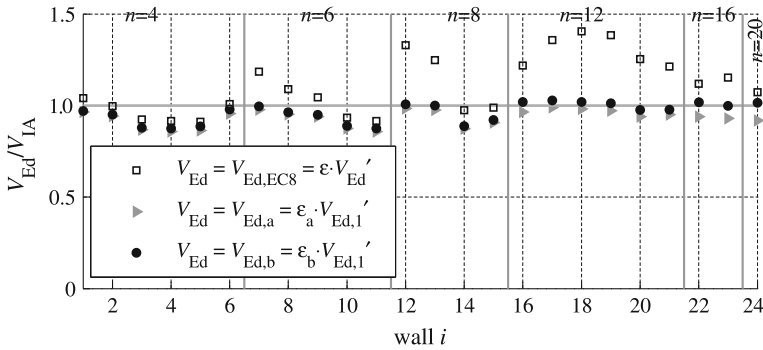


**Fig. 10** Values of  $V_{Ed,EC8}/V_{IA}$  (indicated by square markers),  $V_{Ed,a}/V_{IA}$  (indicated by shaded triangular markers), and  $V_{Ed,b}/V_{IA}$  (indicated by black circular markers) compared to the actual shear magnifications (shown by a grey horizontal line). Each integer on the horizontal axis denotes an analysed wall configuration

$$\varepsilon \cdot V'_{Ed,1} \leq V_E \tag{7a}$$

$$V_E = \varepsilon_{upper} \cdot V'_{Ed,1} = q \sqrt{\left(V'_{Ed,1}\right)^2 + \left(V'_{Ed,2}\right)^2} \tag{7b}$$

By introducing  $V'_{Ed,1}$  into the right hand side of equation 7a, and considering the relation between  $V'_{Ed,1}$  and  $V'_{Ed,2}$  introduced in Sect. 4, the following formulation (8) is obtained for the upper limit  $\varepsilon_{upper}$ :

$$\varepsilon_{upper} = \sqrt{q^2 + 0.1 \cdot \left(q \cdot \frac{S_e(T_C)}{S_e(T_1)}\right)^2} \tag{8}$$

By considering the upper bound for  $\varepsilon$  (Eq. 8), which indicates that the first term under the square root should not be larger than  $q^2$ , a modified formulation for  $\varepsilon_a$  (Eq. 9) is obtained, which should be used in combination with  $V'_{Ed,1}$ :

$$\varepsilon_a = q \cdot \sqrt{\left(\min\left[\frac{\gamma_{Rd}}{q} \cdot \frac{M_{Rd}}{M_{Ed}}; 1\right]\right)^2 + 0.1 \cdot \left(\frac{S_e(T_C)}{S_e(T_1)}\right)^2} \geq 1.5 \tag{9}$$

It is important to note that the value of  $\varepsilon_a$  is not limited by  $q$  and indeed yields values larger than  $q$  for flexible walls ( $T_1 > 2.0$  s).

The shear forces obtained by the corrected shear magnification factor (Eq. 9) are denoted by  $V_{Ed,a}$  ( $V_{Ed,a} = \varepsilon_a \cdot V'_{Ed,1}$ ), and the normalized values  $V_{Ed,a}/V_{IA}$  are shown in Figs. 10, 11, 12 by shaded triangular markers. The new formulation yields good results for the variation of both of the main parameters,  $T_1$  (Fig. 11) and  $\omega$  (Fig. 12).

The procedure only slightly underestimates the shear forces, in particular for walls with higher flexural overstrengths and a significant contribution of the second mode shears  $V'_{Ed,2}$  (more flexible walls). This has suggested that better results will be obtained if a portion of the flexural overstrength is considered also in the second term (under the square root) of Eq. (9), which represents the contribution of the second mode of excitation. This assumption was verified. The coefficient which takes into account the influence of flexural overstrength on the second mode shears  $\omega_{Rd,2}$  (Eq. 10)

$$\omega_{Rd,2} = 1 + A \cdot \left(\frac{\gamma_{Rd} \cdot M_{Rd}}{M_{Ed}} - 1\right) \tag{10}$$

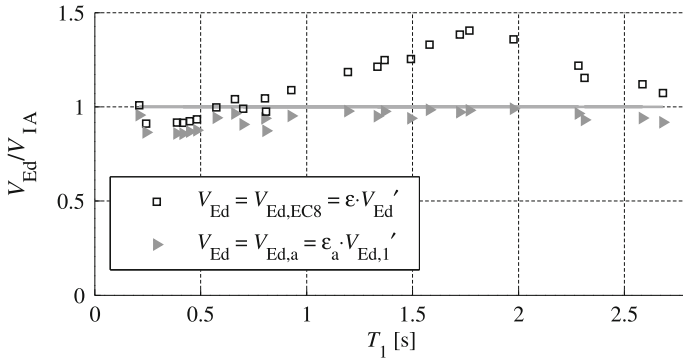


**Fig. 11** Values of  $V_{Ed,EC8}/V_{IA}$  (indicated by *square* markers) and  $V_{Ed,a}/V_{IA}$  (indicated by shaded *triangular* markers) compared to the actual shear magnifications (shown by a *grey horizontal line*) in relation to  $T_1$

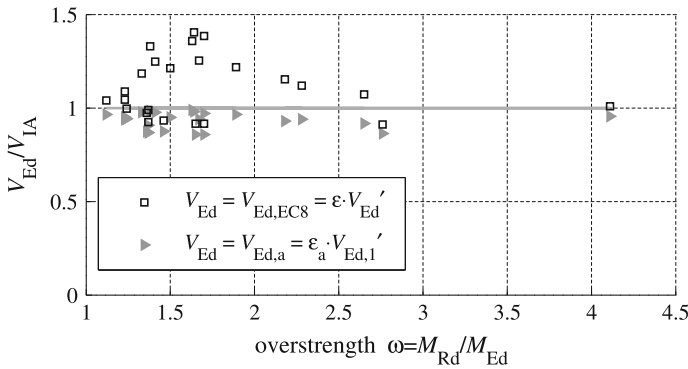


**Fig. 12** Values of  $V_{Ed,EC8}/V_{IA}$  (indicated by *square* markers) and  $V_{Ed,a}/V_{IA}$  (indicated by *grey triangular* markers) compared to the actual shear magnifications (shown by a *grey horizontal line*) in relation to the overstrength factor

was added to the second term of Eq. (9). By means of regression analysis,  $A$  was determined as having a value of 0.07. Using the new modified expression

$$\varepsilon_b = q \cdot \sqrt{\left(\min\left[\frac{\gamma_{Rd}}{q} \cdot \frac{M_{Rd}}{M_{Ed}}; 1\right]\right)^2 + 0.1 \cdot \left(\left(1 + 0.07 \cdot \left(\frac{\gamma_{Rd} \cdot M_{Rd}}{M_{Ed}} - 1\right)\right) \cdot \frac{S_e(T_C)}{S_e(T_1)}\right)^2} \geq 1.5 \tag{11}$$

the results ( $V_{Ed,b} = \varepsilon_b \cdot V'_{Ed,1}$ ; the black circles in Fig. 10) match the results of the inelastic analysis very well. However, the background of this expression has not yet been fully verified, so it will be not discussed in the continuation of this paper.

### 8 Extended study on 72 wall configurations

The research was further extended to a total of 72 cantilever walls in order to investigate wall configurations with more pronounced overstrength factors. In practical design, RC elements are often constructed to have resistance capacities that are considerable higher than

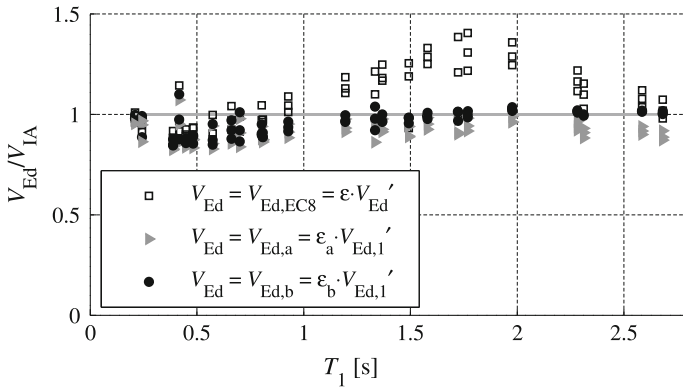


**Fig. 13** Values of  $V_{Ed,EC8}/V_{IA}$  (indicated by square markers),  $V_{Ed,a}/V_{IA}$  (indicated by shaded triangular markers) and  $V_{Ed,b}/V_{IA}$  (indicated by black circular markers) obtained for the 72 walls analysed in the extended study, compared to the actual shear magnifications (shown by a grey horizontal line), in relation to  $T_1$

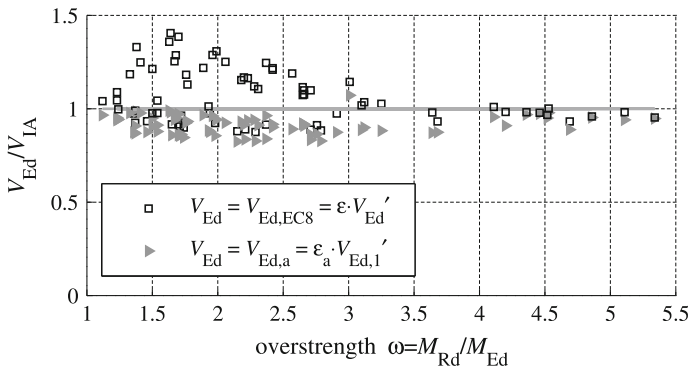


**Fig. 14** Values of  $V_{Ed,EC8}/V_{IA}$  (indicated by square markers) and  $V_{Ed,a}/V_{IA}$  (indicated by shaded triangular markers) obtained for the 72 walls analysed in the extended study, compared to the actual shear magnifications (shown by a grey horizontal line) in relation to the overstrength factor

the demands. For example, a frequent design practice is to neglect the contribution of the longitudinal bars in the web. To consider possible larger overstrengths, the diameter of the reinforcing bars in the boundary areas of the 24 original walls (designed exactly according to the EC8 requirements) was increased in two steps resulting in a total number of 72 walls. Comparisons of the shear forces obtained with the EC8 procedure and with the proposed modified procedure, with the results obtained by means of inelastic response history analyses, are illustrated in Figs. 13 and 14. They reconfirm and more clearly document the conclusions of the basic study.

### 9 Shear force magnifications in DCM walls

The shear magnifications for DCM cantilever walls were also investigated. A similar study (not shown in detail due to the space limitations) to the one performed for the DCH walls reconfirmed (see for example, the paper of Rutenberg and Nsieri 2006) that the uniform

magnification factor  $\varepsilon = 1.5$  provided in EC8 for DCM designed walls is inappropriate and non-conservative.

Although the walls are designed to exhibit moderate inelastic deformations, the amplified effects of the higher modes in the inelastic range are still very pronounced. Moreover, the design procedures and feasibility issues usually result in significant overstrength factors, increasing the shear demands. The analyses have illustrated that the values of the actual magnifications  $V_{IA}/V'_{Ed}$  for the analysed walls lie between 1.5 and 3.0.

The uniform factor  $\varepsilon = 1.5$  was adequate only for the DCM walls ( $q = 3.0$ ) with the first period close to  $T_C$  or less and having low overstrength factors ( $\gamma_{Rd} \approx 1.2$ ). The same conclusion was obtained by using the proposed formula for  $\varepsilon_a$ :

$$\varepsilon_a (q = 3, T_1 \leq T_C, \gamma_{Rd} = 1.2) = 3 \cdot \sqrt{(\min [ \frac{1.2}{3}; 1 ])^2 + 0.1 \cdot (1.0)^2} = \underline{1.53} \quad (12)$$

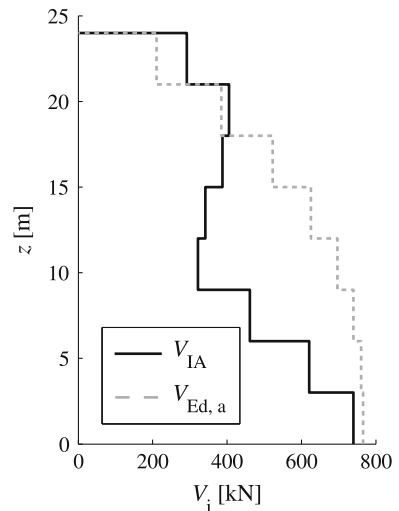
The authors therefore suggest the use of the modified procedure proposed for DCH walls in this paper in the case of DCM walls, too.

### 10 Seismic shear demand along the height of the walls

Although Keintzel’s equation was derived only for the estimation of the base shear in multi-storey cantilever walls, Eurocode 8 applies the same magnification factor over the entire height of the wall. In this section it will be shown that this requirement leads to non-optimal and in some cases even unsafe design.

It should be recalled that the derivation of the shear magnification factor  $\varepsilon$  is based on the assumed ratio between the second mode (higher modes) and first mode contributions to the (base) shear force. This ratio was assumed to be equal to:  $0.3 \cdot S_e(T_2)/S_e(T_1)$ . Figure 17c in “Appendix” shows that in the elastic region this ratio varies considerably along the height of the wall, being much smaller at the mid-height and much larger at the top of the wall. Very similar trends were observed in the results of the inelastic response. An example corresponding to one of the analysed 8-storey walls ( $l_w = 3.0$  m,  $A_w/A_f = 1.5\%$ ) is shown in Fig. 15.

**Fig. 15** Comparison of seismic shears obtained by inelastic response history analyses  $V_{IA}$  with the design shears  $V_{Ed,a} = \varepsilon_a \cdot V'_{Ed,1}$  for a typical 8 storey wall ( $l_w = 3.0$  m,  $A_w/A_f = 1.5\%$ )





The idea has therefore been that Keintzel’s magnification factor could be used along the entire height of the wall, providing that the constant ratio between the contribution of the higher modes to the contribution of the first mode is replaced by a variable ratio along the height (Eq. 13):

$$\varepsilon_a(z) = q \cdot \sqrt{\left(\min\left[\frac{\gamma_{Rd}}{q} \cdot \frac{M_{Rd}}{M_{Ed}}; 1\right]\right)^2 + m(z)^2 \cdot \left(\frac{S_e(T_C)}{S_e(T_1)}\right)^2} \geq 1.5 \tag{13}$$

The same distribution  $m(z)$  of this ratio as in the case of the elastic flexural cantilever beam (Fig. 17c in “Appendix”) was chosen, fully realizing that this is only an approximation in the inelastic range and is applicable only to regular walls with no plastic hinges in the upper stories.

The results  $V_{Ed,a}(z)$  obtained by using  $\varepsilon_a(z)$  in combination with  $V'_{Ed,1}$  are presented, for some selected configurations of the analysed walls, in Fig. 16. The results are compared

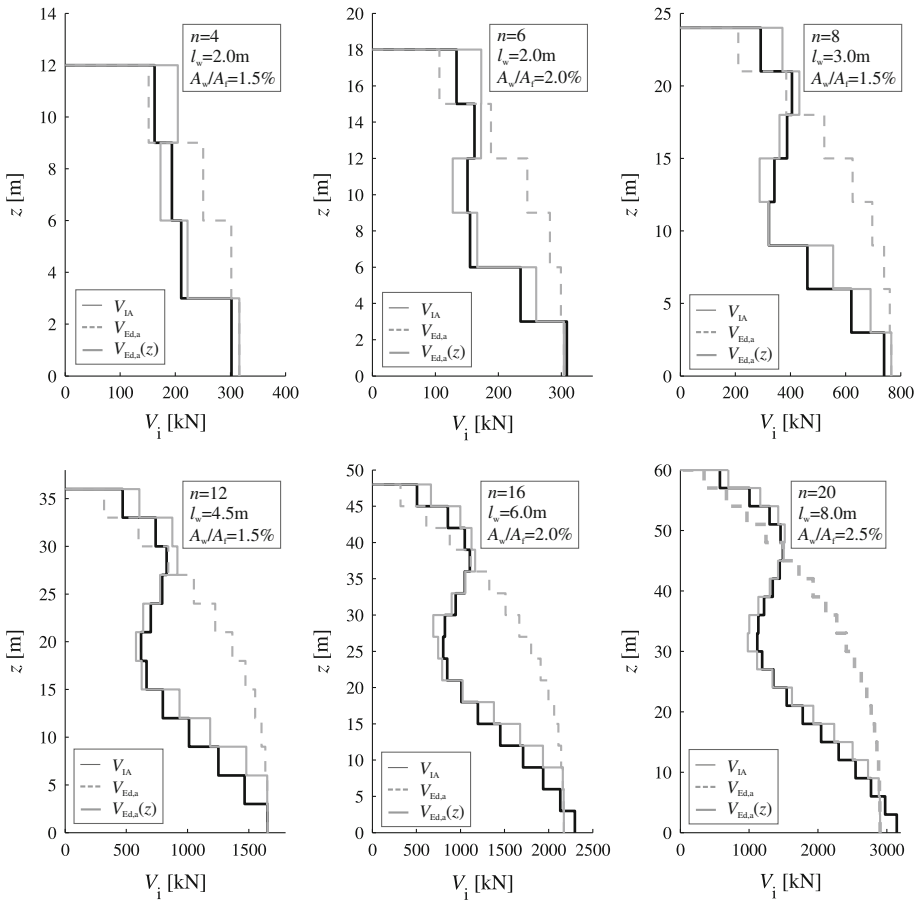


**Fig. 16** The results obtained by using  $V_{Ed,a}(z) = \varepsilon_a(z) \cdot V'_{Ed,1}$  (indicated by a grey line) for 6 selected configurations of the analysed walls compared with the shear envelopes obtained by means of inelastic response history analyses  $V_{IA}$  (indicated by a black line) and the design shears obtained by the basic method  $V_{Ed,a} = \varepsilon_a(z) \cdot V'_{Ed,1}$  (indicated by a dashed grey line)

with the shear envelopes obtained by using inelastic response history analyses  $V_{IA}$  and the design shears obtained by multiplying  $V'_{Ed,1}$  with  $\varepsilon_a(z=0)$  along the entire height (the basic method).

Figure 16 shows that the proposed modification of the procedure yields a very good match over the entire height of the wall. Similarly good results were obtained for all of the 72 analysed walls. It is therefore believed that the proposed procedure enables optimum and safe design over the entire height of the wall.

## 11 Conclusions

1. Inelastic dynamic magnification of seismic shear forces in multi-storey cantilever walls has been discussed in the paper. An extensive parametric study was performed in order to determine the reliability of the procedure in Eurocode 8. A large number of single cantilever walls characteristic for the design practice in Europe and designed to conform to all EC8 requirements were analysed. The results obtained with the (modified) code procedures were compared with the results of the inelastic response history analyses.
2. Large shear magnification factors (up to the value of the behaviour factor  $q$ ) were re-confirmed, although they are questioned by many design practitioners and researchers. In addition to the large magnifications caused by the amplified effect of the higher modes in the inelastic range, the flexural overstrength inherent in the EC8 design provisions further increases the shear demands.
3. The procedure provided in Eurocode 8 to determine seismic shear magnification in DCH cantilever walls is based on the expression proposed by Keintzel (1990). If properly applied, this procedure usually yields acceptable (even very good) results for base shears. However, as presently formulated and understood in EC8, it can yield significantly incorrect results (overestimated by up to 40%), in particular in the case of mid-period walls ( $1.0\text{ s} < T_1 < 2.5\text{ s}$ ). The results for very flexible walls appear adequate, but this is the result of two errors cancelling each other out. So the following modifications of the EC8 procedure are proposed:
  - (3a) Keintzel's formula should be used in combination with the seismic shears obtained by considering the first mode of excitation only. Since EC8 does not specify this requirement, designers typically follow the established practice with standard programs that take into account all the important modes. In the case of flexible buildings (walls), where the contribution of the higher modes is important even in the elastic range, this would yield conservative results.
  - (3b) The upper limit of the  $\varepsilon$  factor should be related to the total shear force (not only to the shear force due to the first mode as assumed in Keintzel's original formula).

These two improvements could be achieved with only a slightly modified shear magnification factor (the parameters are defined in the main body of the text and in EC8), which should be used in combination with shear forces determined by considering the fundamental mode only:

$$\varepsilon_a = q \cdot \sqrt{\left(\min\left[\frac{\gamma_{Rd}}{q} \cdot \frac{M_{Rd}}{M_{Ed}}; 1\right]\right)^2 + 0.1 \cdot \left(\frac{S_e(T_C)}{S_e(T_1)}\right)^2} \geq 1.5$$

4. Very good results were obtained when using the modified shear magnification factor and procedure. Apart from a consideration of the analytical background of the procedure, the

- authors prefer this (modified) method when compared to some other purely empirical procedures that have been proposed in the literature.
5. It was reconfirmed that the constant shear magnification factor  $\varepsilon = 1.5$ , which is used in EC8 for DCM structures, is typically too low (values of up to 3 were demonstrated by the inelastic analysis). It is strongly recommended that the same procedure as required for DCH walls be used also for DCM walls.
  6. The shear magnification factor defined in EC8 as well as the proposed modified factor ( $\varepsilon_d$ ) are valid for the base shear only. This magnification for the base shear is conservative at the mid-height of the wall and might be unsafe at the top of the wall. Variable shear magnification factor along the height of the wall has been proposed and successfully tested.

**Acknowledgments** The results presented in this paper are based on work supported by the Slovenian Research Agency. This support is hereby gratefully acknowledged.

**Appendix: Shear forces and bending moments in an elastic flexural cantilever beam**

For the purpose of the analysis and derivations in this paper, it has been practical to represent a slender cantilever shear wall in a mid-rise building by a flexural cantilever beam with a distributed mass  $m$  and a height  $H$ . The distribution of elastic shear forces and bending moments along the height of the cantilever can then be obtained in a closed form by the standard modal spectrum analysis of continuous elastic systems (i.e. Fajfar 1984). The moment  $M_i(\bar{z})$  and the shear force  $V_i(\bar{z})$  at the height  $\bar{z} = z/H$  ( $z$  is the vertical coordinate—see Fig. 15) due to the  $i$ th mode are expressed as

$$M_i(\bar{z}) = m \cdot H^2 \cdot S_d(T_i) \cdot \bar{M}_i(\bar{z}) \tag{14}$$

$$V_i(\bar{z}) = m \cdot H \cdot S_d(T_i) \cdot \bar{V}_i(\bar{z}) \tag{15}$$

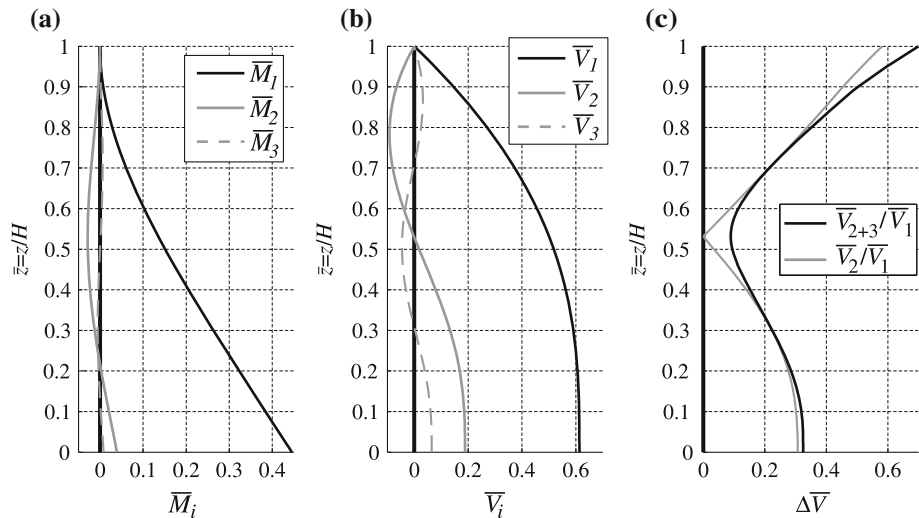


**Fig. 17** The distribution of the normalized bending moments (a) and the normalized shear forces (b) along the height of the cantilever; (c) the ratio of the second/higher modes normalized shear to the first mode normalized shear

where  $S_d(T_i)$  is the ordinate of the elastic acceleration design spectrum at the period  $T_i$ . The normalized functions  $\bar{M}_i(\bar{z})$  and  $\bar{V}_i(\bar{z})$  are shown in Figs. 17a, b, respectively. For shear forces, the ratio of the second mode contribution to the first mode contribution is shown by means of a grey solid line in Fig. 17c. The ratio of the combined second and third mode contribution (roughly equal to the contribution of all higher modes) to the first mode contribution is shown by means of a black solid line.

It can be observed that:

- (a) the contribution of higher modes to the bending moment at the base is negligible;
- (b) the ratio of the second mode shear to first mode shear at the base is about  $0.3 \approx \sqrt{0.1}$ ;
- (c) the ratio of the higher and first mode shear varies considerably along the height of the cantilever.

## References

- Blakeley RWG, Cooney RC, Megget LM (1975) Seismic shear loading at flexural capacity in cantilever wall structures. *Bull New Zeal Natl Soc Earthq Eng* 8(4):278–290
- CEN (2004) Eurocode 8—design of structures for earthquake resistance. Part 1: General rules, seismic actions and rules for buildings. European standard EN 1998-1, December 2004, European Committee for Standardization, Brussels
- CEN (2005) Eurocode 2—design of concrete structures—Part 1-1: General rules and rules for buildings. European standard EN 1992-1-1:2004, May 2005, European Committee for Standardization, Brussels
- CSI (2009) ETABS extended 3D analysis of building Systems. Computers and Structures Inc, Berkeley
- Fajfar P (1984) *Dinamika gradbenih konstrukcij* (Dynamics of building structures). Faculty of Civil Engineering, Architecture and Geodesy, University of Ljubljana, Slovenia
- Fardis MN (2009) *Seismic design, assessment and retrofitting of concrete buildings based on EN-Eurocode 8*. Springer Dordrecht, Heidelberg. doi:10.1007/978-1-4020-9842-0
- Kappos AJ, Antoniadis P (2007) A contribution to seismic shear design of R/C walls in dual structures. *Bull Earthq Eng* 5:443–466. doi:10.1007/s10518-007-9041-6
- Keintzel E (1990) Seismic design shear forces in RC cantilever shear wall structures. *Eur Earthq Eng* 3:7–16
- Naumoski ND (1998) Program SYNTH, Generation of artificial accelerograms compatible with a target spectrum
- OpenSees (2008) Pacific Earthquake Engineering Research Center, University of California, Berkeley. <http://opensees.berkeley.edu>. Cited 8 July 2010
- Panagiotou M, Restrepo JJ, Conte JP (2007) Shake table test of a 7 story full scale reinforced concrete structural wall building slice phase I: Rectangular Wall Section, SSRP 07-07 Report. Department of Structural Engineering, University of California San Diego
- Priestley MJN, Calvi GM, Kowalsky MJ (2007) *Displacement-based seismic design of structures*. IUSS PRESS, Pavia
- Rutenberg A, Nsieri E (2006) The seismic shear demand in ductile cantilever wall systems and the EC8 provisions. *Bull Earthq Eng* 4:1–21. doi:10.1007/s10518-005-5407-9